



 Cite this: *RSC Adv.*, 2026, 16, 26421

# Nitrate removal by acid-tolerant *Fictibacillus phosphorivorans* MJ9 in acidic anaerobic environments

 Jing Zhang,<sup>†a</sup> Feifei Wang,<sup>†a</sup> Min Ai,<sup>†b</sup> Xiafei Yin,<sup>†c</sup>  <sup>\*a</sup> Lixue Liu,<sup>a</sup> Hefei Shi<sup>\*a</sup> and Guobin Liang<sup>ac</sup>

In this study, an acid-tolerant strain, *Fictibacillus phosphorivorans* MJ9, demonstrated exceptional nitrate removal efficiency under acidic conditions. It achieved  $80.4 \pm 1.1\%$  nitrate degradation at an initial pH of 3.1. Metabolomic and proteomic analyses suggest that nitrate reduction by strain MJ9 primarily occurs *via* dissimilatory nitrate reduction to ammonium (DNRA) and partial denitrification, accompanied by incomplete denitrification. In addition, key metabolic processes—including glycolysis, fatty acid metabolism, purine metabolism, and the tricarboxylic acid (TCA) cycle—play essential roles in supplying energy, regulating metabolic fluxes, and maintaining cellular homeostasis. Collectively, these findings underscore the remarkable nitrate removal capability of the novel strain MJ9 and provide valuable insights into its metabolic adaptations under anaerobic and acidic conditions.

Received 9th February 2026

Accepted 4th May 2026

DOI: 10.1039/d6ra01143h

[rsc.li/rsc-advances](https://rsc.li/rsc-advances)

## 1 Introduction

Excessive nitrate contamination of groundwater (greater than  $45 \text{ mg L}^{-1}$ ) has been detected in countries such as China, Thailand, and India, affecting tens of millions of people each year.<sup>1</sup> This pollution, primarily driven by the overuse of nitrogen fertilizers and industrial emissions, is intensifying globally.<sup>2,3</sup> Beyond environmental consequences such as eutrophication and reduced dissolved oxygen,<sup>4</sup> the conversion of nitrate to nitrite in the human body impairs hemoglobin's oxygen-carrying capacity, leading to serious health risks including cancer and methemoglobinemia.<sup>5</sup> Therefore, developing low-cost and efficient technologies for treating high-nitrate wastewater is critical for environmental protection and public health.

Compared to physical or chemical methods, biological methods are more economical and effective in removing nitrates from wastewater without the risk of secondary contamination.<sup>6</sup> The conventional biological nitrogen removal method is divided into two stages—nitrification and denitrification—which inevitably increases operating costs. Additionally, autotrophic nitrifying bacteria grow slowly and are susceptible to fluctuations in effluent composition, limiting the

efficiency and applicability of conventional biological nitrogen removal methods.<sup>7</sup> An alternative solution is the use of heterotrophic nitrifying and aerobic denitrifying (HNAD) bacteria, as they can simultaneously perform both nitrification and denitrification under aerobic conditions and exhibit faster growth rates. However, their nitrogen removal efficiency may be significantly reduced under harsh environmental conditions, such as high osmotic pressure, which could lead to excessive accumulation of nitrite and nitrous oxide, as well as cell dehydration and death.<sup>8</sup> Similarly, anaerobic ammonia oxidation (anammox) is a promising strategy for the treatment of saline wastewater. However, its efficiency is limited by high organic loads, temperature fluctuations, and slow microbial growth, which pose challenges to its widespread application.<sup>9</sup> Furthermore, both nitrification-denitrification and ammonia oxidation processes ultimately result in nitrogen loss.<sup>10</sup>

The ability of microorganisms to remove nitrogen is influenced by various environmental factors, with pH playing a crucial role in microbial growth, metabolism, and enzymatic activity. Most HNAD bacteria perform optimally in neutral to alkaline environments.<sup>11</sup> For example, strains such as *Halomonas* sp. DN3 and *Pseudomonas fragi* EH-H1 have demonstrated efficient removal of ammonium, nitrate, and nitrite at pH 7.2.<sup>12,13</sup> Similarly, *P. aryabhatai* KX-3 has been shown to eliminate 92.5% of ammonium, 96.0% of nitrate, and 56.7% of nitrite at pH 10.<sup>14</sup> In contrast, strains like *Acinetobacter* sp. C-13,<sup>15</sup> and *Acinetobacter indicus* ZJB20129 (ref. 16) exhibited weak nitrification and denitrification at pH values below 6.0. The value of pH significantly affects cell membrane permeability and enzyme activity.<sup>17</sup> The denitrifying enzymes present in HNAD microorganisms are sensitive to pH, and extreme pH

<sup>a</sup>School of Resources and Environmental Engineering, Jiangsu University of Technology, Changzhou 213001, P. R. China. E-mail: yinxiafei@jsut.edu.cn; shifeifei@jsut.edu.cn

<sup>b</sup>Consulting Department, Jiangsu Longheng Environmental Technology Co., Ltd, Changzhou, P. R. China

<sup>c</sup>School of Chemistry and Chemical Engineering, Jiangsu University of Technology, Changzhou 213001, P. R. China

<sup>†</sup> These authors contributed to the work equally and should be regarded as co-first authors.



levels can inhibit their activity or even lead to their inactivation.<sup>18</sup> The studies mentioned above suggest that certain limitations may arise when using conventional microorganisms for the treatment of acidic wastewater from industries such as mining, metallurgy, and pharmaceuticals.

Despite the existence of several acid-tolerant bacterial strains, the underlying molecular mechanisms enabling efficient nitrate reduction under highly acidic (pH < 4.0) and anaerobic conditions remain poorly elucidated. Unlike previously reported acid-tolerant denitrifiers that operate at pH  $\geq$  5.0, strain MJ9 maintains nitrate reduction at pH 3.1—a proton concentration 100–1000 times higher—representing a more extreme case of acidophilic nitrate reduction. Most previous studies have focused on phenotypic characterization at near-neutral or mildly acidic pH (5.5–6.5),<sup>19</sup> leaving a critical knowledge gap under more extreme acidic conditions. Recent advances have begun to shed light on acid adaptation strategies in denitrifying bacteria.<sup>20</sup> Key findings include enhanced glutamate decarboxylase activity, accumulation of compatible solutes, and upregulation of stress-response proteins to maintain intracellular pH and redox balance. However, these studies have primarily focused on pH thresholds above 4.0, and the specific molecular responses to combined extreme acidity (pH < 4.0) and anoxia remain largely unexplored. To address this, we employed an integrated metabolomic and proteomic approach. These powerful techniques allow for a system-level understanding of the metabolic fluxes and stress responses, moving beyond mere correlation to reveal causative mechanisms, as demonstrated in recent studies on microbial stress adaptation.<sup>21</sup> Therefore, the objectives of this study were to: (1) isolate and identify a novel, highly acid-tolerant nitrate-reducing bacterium; (2) optimize its nitrate removal efficiency under acidic, anaerobic conditions; and (3) elucidate the key metabolic pathways and proteomic profiles responsible for its nitrate removal capability and acid tolerance.

## 2 Materials and methods

### 2.1. Culture medium and reagents

Luria–Bertani (LB) medium is included (per liter): 10 g Tryptone, 5 g yeast extract, 10 g NaCl. Agar powder, H<sub>2</sub>SO<sub>4</sub>, HCl, and NaOH were purchased from Sinopharm Chemical Reagent Co., Ltd (Shanghai, China). All reagents utilized were of analytical grade.

### 2.2. Isolation and identification

Isolation of a novel nitrate-degrading bacterium (MJ9) from activated sludge of a wastewater treatment plant by gradient dilution and plate scribing.<sup>22</sup> The morphology of the MJ9 was observed through a microscope (Olympus CX33, Japan). Genomic DNA was extracted, and the 16S rDNA gene was amplified *via* polymerase chain reaction (PCR) using universal primers 27F (5'-AGAGTTTGATCCTACTCAG-3') and 1492R (5'-GGTTACCTTGTTTCAGACTT-3'). The PCR was performed under the following conditions: initial denaturation at 94 °C for 5 min; followed by 30 cycles of denaturation at 94 °C for 30 s, annealing at 55 °C for 30 s, and extension at 72 °C for 90 s; with a final

extension at 72 °C for 10 min. The PCR products were purified and sequenced using the Sanger sequencing platform by Shanghai Sangon Biotech Co., Ltd (Shanghai, China). The obtained 16S rDNA sequences were aligned against the GenBank database using BLAST (<https://blast.ncbi.nlm.nih.gov/Blast.cgi>), and strains with sequence similarity greater than 98% were considered as the same species. A neighbor-joining phylogenetic tree based on 16S rDNA sequences was constructed using MEGA 11.0 software, to evaluate the phylogenetic relationship between MJ9 and other reference strains.<sup>23</sup>

### 2.3. Experimental methods

The acid washing wastewater in this experiment comes from a factory in Changzhou. The wastewater contains a large amount of organic and inorganic pollutants, such as heavy metals (Fe<sup>3+</sup>, Cu<sup>2+</sup>), salts (nitrates), *etc.* The detailed chemical composition of the raw pickling wastewater is summarized in Table 1. The pH is 3.1 and the nitrate nitrogen (NO<sub>3</sub><sup>-</sup>-N) content is 11.8 ± 0.3 mg L<sup>-1</sup>. To investigate the effect of carbon source and improve the carbon-to-nitrogen (C/N) ratio, a separate set of experiments was conducted where filter-sterilized glucose was added as an external carbon source to a final concentration of 2 g L<sup>-1</sup> at the beginning of the incubation. The initial C/N ratio of the wastewater was calculated to be approximately 5.3 (based on TOC and NO<sub>3</sub><sup>-</sup>-N), and the addition of glucose adjusted it to approximately 67.8.

The bacterium MJ9 was inoculated at 2% v/v into 100 mL of LB medium and cultured to a logarithmic phase of growth. The bacterial culture was grown to a standardized optical density (OD<sub>600</sub> ≈ 1.5). Then, 10 mL, 30 mL, 50 mL, 70 mL, 90 mL and 110 mL of this culture were centrifuged, and the resulting cell pellets were separately resuspended and added to 100 mL of wastewater, yielding different initial biomass concentrations proportional to the centrifugation volume. The bacterial solution was centrifuged to separate the bacteria from the liquid, and the resulting bacteria were then placed into 100 mL of wastewater for biodegradation. Anaerobic incubation was performed for 72 h. Regularly take samples to determine the content of TN, NO<sub>3</sub><sup>-</sup>-N, NO<sub>2</sub><sup>-</sup>-N, and NH<sub>4</sub><sup>+</sup>-N during incubation.

Table 1 Chemical characterization of the raw pickling wastewater

Parameter	Concentration (mg L <sup>-1</sup> )
pH	~3.0
F <sup>-</sup>	11.10
Cl <sup>-</sup>	0.09
NO <sub>2</sub> <sup>-</sup>	0.13
NO <sub>3</sub> <sup>-</sup>	52.22
CO <sub>3</sub> <sup>2-</sup>	3.69
SO <sub>4</sub> <sup>2-</sup>	0.18
C <sub>2</sub> O <sub>4</sub> <sup>2-</sup>	0.57
NH <sub>4</sub> <sup>+</sup>	0.17
Ca <sup>2+</sup>	0.86
Fe	6.09
Cr	0.85
Ni	1.58
Cu	0.01



For all nitrate removal experiments, sterile controls (without bacterial inoculation) were included in parallel to account for any chemical or physical loss of nitrate under the experimental conditions. All the above experiments are conducted in triplicate. No significant nitrate reduction was observed in these abiotic controls.

## 2.4. Analytical methods

The changes in the concentrations of nitrates ( $\text{NO}_3^-$ -N) and total nitrogen (TN) were measured according to the Chinese State Environment Protection Agency (SEPA) standard methods.<sup>24</sup>  $\text{NO}_2^-$ -N was determined by the spectrophotometric method using *N*-(1-naphthyl)-ethylenediamine (GB 7493-87), and  $\text{NH}_4^+$ -N was determined by Nessler's reagent spectrophotometry (HJ 535-2009). A microplate reader (Infinite 200PRO, Beijing Longyue Biotechnology Development Co., Ltd, Beijing, China) was used to measure  $\text{OD}_{600}$  value (as shown in section 1). The database for identification of differential metabolites was KEGG.<sup>25</sup> Volcano plot analysis and metabolic pathway analysis were performed using MetaboAnalyst 5.0.<sup>26</sup>

All data points in Fig. 2 represent the mean  $\pm$  standard deviation (SD) of three independent biological replicates ( $n = 3$ ). Statistical significance between different inoculum doses at the 72-hour time point was determined by one-way ANOVA followed by Tukey's post-hoc test, with  $p < 0.05$  considered significant.

## 2.5. Metabolomics and proteomics analysis

**2.5.1. Metabolomics.** After 72 hours of incubation, cells from the 110 mL inoculum condition and a zero-time point control were rapidly quenched and harvested. Intracellular metabolites were extracted using a methanol/acetonitrile/water system. The extracts were analyzed using a UHPLC-Q-TOF MS system (Thermo Orbitrap Exploris 120) in both positive and negative ionization modes. Raw data were processed with Xcalibur and subsequent bioinformatics tools for peak picking, alignment, and normalization. Metabolites were identified by matching against the KEGG and HMDB databases. The identification confidence level was set as Level 2 (putatively annotated compounds based on accurate mass and MS/MS spectral matching). Three independent biological replicates were

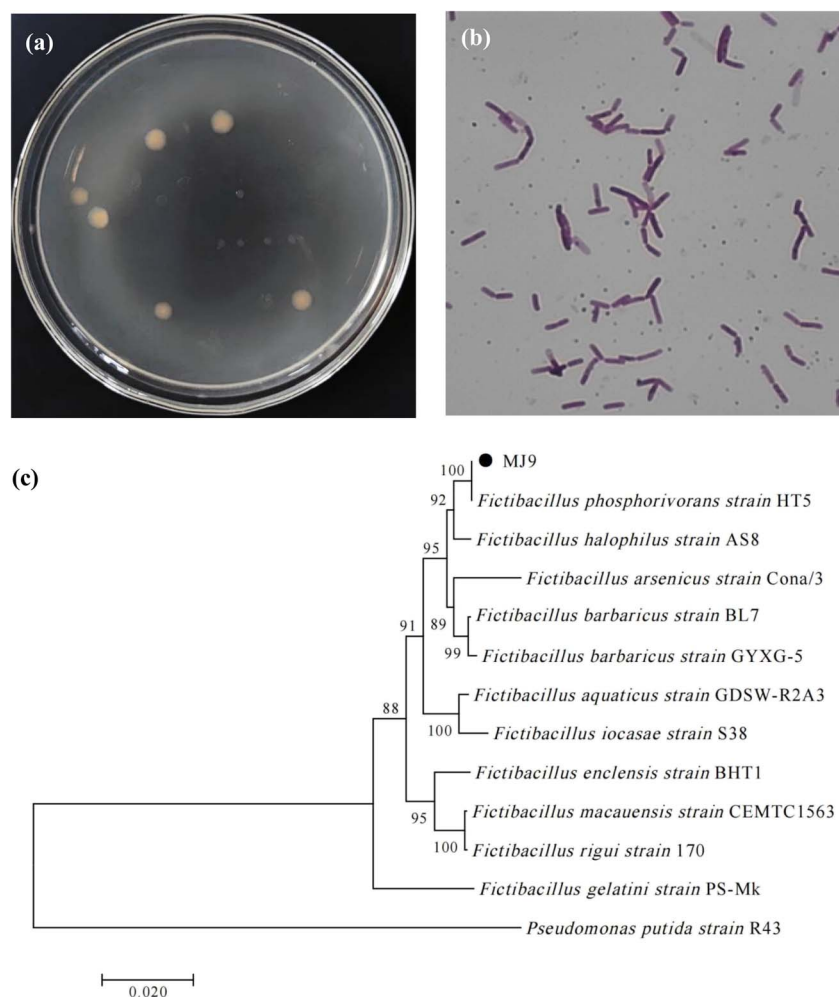


Fig. 1 (a) Morphological characteristics of colony morphology. (b) Gram Staining. (c) Phylogenetic tree based on neighbor linkage analysis of partial 16S rDNA gene sequences.



performed for each condition, and a pooled quality control (QC) sample was injected every 10 samples to monitor instrument stability. Significantly differential metabolites were screened with a VIP > 1.0 (from OPLS-DA model) and a *p*-value < 0.05.

**2.5.2. Proteomics.** Total proteins were extracted from cell pellets using SDT lysis buffer. Protein digestion was performed using trypsin. The resulting peptides were analyzed by nano-LC-MS/MS. The MS data were searched against the *Lysinibacillus* sp. or *Fictibacillus phosphorivorans* protein database using a standard proteomics search engine with a false discovery rate (FDR) of < 1%. Three biological replicates were analyzed for each condition. Proteins with a fold change > 1.5 or < 0.67 and a *p*-value < 0.05 were considered differentially expressed.

## 3 Results and discussion

### 3.1. A novel nitrate degrading bacterium MJ9 and its degradation characteristics

**3.1.1. Isolation and characterization of MJ9.** As shown in Fig. 1a, the colonies of MJ9 were yellowish, with a moist, opaque surface and clear margins. MJ9 was characterized as Gram-

negative (Fig. 1b), and the bacteria appeared rod-shaped under the light microscope. Homology analysis using BLAST revealed that the MJ9 strain was most similar to *Fictibacillus phosphorivorans*, with a 99.74% similarity. The constructed phylogenetic tree (Fig. 1c) confirmed that MJ9 belongs to the genus *Fictibacillus*. Therefore, MJ9 was initially identified as *Fictibacillus phosphorivorans*.<sup>27</sup> The MJ9 strain is preserved in the China Center for Type Culture Collection (CCTCC no. 28762).

**3.1.2. Degradation characteristics of MJ9 on high nitrate pickling wastewater.** As shown in Fig. 2a, the OD<sub>600</sub> values exhibited a decreasing trend within the first 24 hours under anaerobic conditions, likely due to environmental stress affecting the growth and metabolism of the strains. However, in the treatments with bacterial dosages of 50 mL, 70 mL, 90 mL, and 110 mL, OD<sub>600</sub> values significantly increased after 24 hours. This suggests that the higher initial inoculum provided more active bacteria, facilitating a faster adaptation and recovery process. During optimization of the culture conditions, it was observed that the OD<sub>600</sub> values of strain MJ9 gradually increased under static conditions (0 rpm), indicating that once the strain

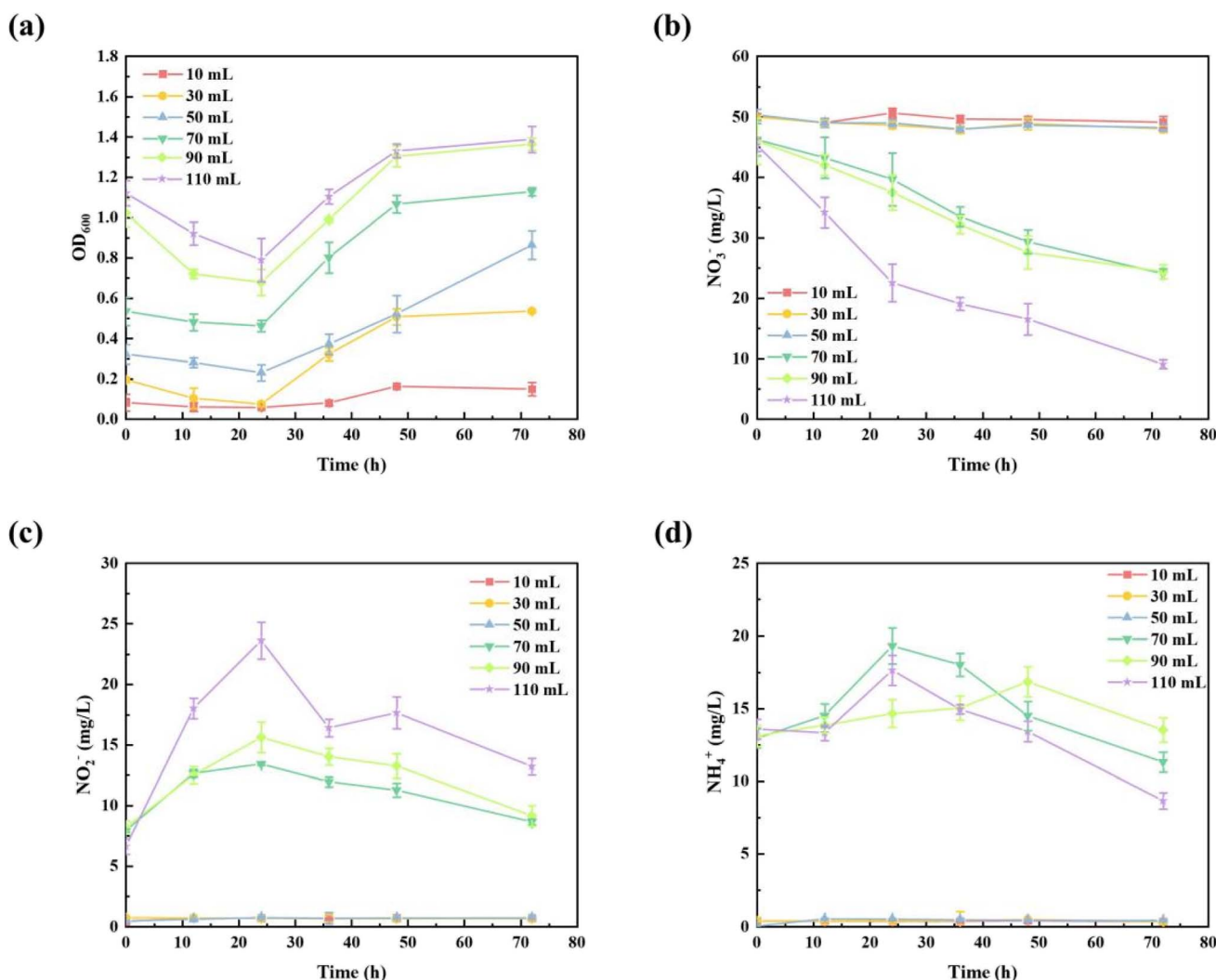


Fig. 2 Changes in OD<sub>600</sub> (a), NO<sub>3</sub><sup>-</sup>-N content (b), NO<sub>2</sub><sup>-</sup>-N content (c), and NH<sub>4</sub><sup>+</sup> (d) of wastewater with different bacterial strains dosage.



adapted to the anaerobic environment, cell density tended to rise steadily. Pretreatment with different bacterial dosages led to considerable variation in pH. When the dosage was 10 mL, 30 mL, or 50 mL, the pH of the wastewater dropped below 4 (as shown in Fig. S1a). It is evident that at these lower dosages, the pH remained largely unchanged over time, and no significant nitrate reduction was observed, similar to the abiotic controls. This may be attributed to the acidic conditions (pH < 4), which likely inhibited the metabolic activity of strain MJ9. In contrast, as shown in Fig. 2b, higher dosages (70 mL, 90 mL, and 110 mL) resulted in nitrate (NO<sub>3</sub><sup>-</sup>-N) reductions of 47.9 ± 1.2%, 46.9 ± 1.9%, and 80.4 ± 1.1% after 72 hours, respectively, which were attributed to bacterial activity as no such reduction occurred in the abiotic controls. Although the 90 mL and 110 mL treatments did not reach a complete plateau by 72 hours, the nitrate concentrations continued to decline steadily, suggesting that the reaction was still ongoing. The 70 mL treatment showed minimal change after 48 hours, indicating an early quasi-plateau. These findings indicate that strain MJ9 cannot fully reduce nitrate under the current conditions within the 72-hour timeframe, likely due to limitations imposed by low pH and carbon availability. A higher density of active colonies may enhance the activation of acid stress response mechanisms, thereby improving the metabolic stability of the strain in harsh environments.<sup>28</sup> Although strain MJ9 demonstrated effective nitrate removal, transient accumulation of nitrite (NO<sub>2</sub><sup>-</sup>-N) and persistent low levels of ammonia (NH<sub>4</sub><sup>+</sup>-N) were observed, as shown in Fig. 2c and d. Notably, nitrite levels peaked at 10–30 hours and then decreased, while a small amount of ammonium remained at the end of the experiment. Given that the carbon-to-nitrogen ratio had been optimized with glucose supplementation (2 g L<sup>-1</sup>), this pattern is unlikely to result from carbon limitation. Instead, it suggests the possible coexistence of denitrification and dissimilatory nitrate reduction to ammonium (DNRA) pathways under acidic anaerobic conditions, or a temporary imbalance between nitrate and nitrite reduction rates. Notably, a moderate amount of glucose (2 g L<sup>-1</sup>) was added as an external carbon source in this experiment to support microbial activity.<sup>29</sup> As shown in Fig. S1b, at low inoculum volumes (10 mL and 30 mL), total organic carbon (TOC) levels increased, possibly due to bacterial cell lysis and the release of intracellular contents. At a dosage of 50 mL, TOC showed a significant decline, indicating that carbon-containing compounds were being effectively consumed or degraded by the microorganisms. This suggests that strain MJ9 remained

metabolically active under these conditions.<sup>30</sup> The TOC degradation efficiencies at bacterial dosages of 50 mL, 70 mL, 90 mL, and 110 mL were 24.8 ± 0.8%, 21.4 ± 3.3%, 41.5 ± 1.7%, and 54.9 ± 2.0%, respectively.

In this study, the NO<sub>3</sub><sup>-</sup>-N removal efficiency of MJ9 (80.4 ± 1.1%) was higher than that of *Bacillus simplex* H-b (67.29%) reported by Yang<sup>31</sup> *et al.* Additionally, as shown in Table 2, MJ9 demonstrated more stable removal performance at 35 °C, maintaining a rate of 80.4 ± 1.1% over 72 hours. In contrast, the removal rate of *Pseudomonas stutzeri* YG-24 (ref. 32) was lower, at only 70.83%, while MJ9 showed higher NO<sub>3</sub><sup>-</sup>-N degradation efficiency under similar conditions. Furthermore, MJ9 also outperformed *Acinetobacter* sp. JR1 (68.3%), as reported by Yang<sup>33</sup> *et al.*, which exhibited lower removal efficiency. Although *Comamonas* sp. pw-6 achieved a high NO<sub>3</sub><sup>-</sup>-N removal efficiency of 89.84% in the study by Chen<sup>34</sup> *et al.*, its reaction requires succinate as a carbon source, leading to higher energy and resource consumption. Therefore, the findings of this study suggest that optimizing strain dosing could effectively enhance NO<sub>3</sub><sup>-</sup>-N degradation efficiency.

### 3.2. Metabolomic analysis

OPLS-DA with VIP > 1 and *P* value < 0.05 was used as the criteria for screening metabolites with significant differences in metabolomics. As shown in Fig. 3a, a total of 928 metabolites were identified, with 321 metabolites upregulated and 607 metabolites downregulated after the metabolism of strain MJ9. During the experiment, as illustrated in Fig. 3b, the upregulated metabolites were likely produced as a result of the reaction, while the downregulated metabolites were likely consumed during the process.

The observed accumulation of ammonia and residual nitrogen in the treated wastewater (Fig. 2c and d) is consistent with the transient nitrite profile and further supports the occurrence of DNRA or incomplete denitrification under the tested acidic anaerobic conditions. As shown in Fig. 2d, a low but persistent level of ammonium (NH<sub>4</sub><sup>+</sup>-N) remained at the end of the experiment (72 h), accompanied by transient nitrite accumulation peaking at 10–30 h (Fig. 2c). This pattern indicates enhanced dissimilatory nitrate reduction to ammonium (DNRA) activity, where, under anaerobic conditions, nitrate is reduced to ammonia rather than being fully converted to nitrogen gas. To investigate the reduction mechanism of strain MJ9, metabolic differentiators were compared before and after treatment. In glycolytic metabolism, glucose, as a readily

Table 2 Efficiency of NO<sub>3</sub><sup>-</sup>-N-containing wastewater degradation by different bacterial strains

Bacteria	NO <sub>3</sub> <sup>-</sup> -N concentration of initial wastewater (mg L <sup>-1</sup> )	Degradation conditions	Degradation efficiency	References
<i>Bacillus simplex</i> H-b	63.0	168 h, 10 °C	67.29%	(Yang <i>et al.</i> , 2021)
<i>Pseudomonas stutzeri</i> YG-24	100	50 h, 25~35 °C, 150 rpm	70.83%	(Li <i>et al.</i> , 2015)
<i>Acinetobacter</i> sp. JR1	51.6	48 h, 30 °C, 120 rpm	68.3%	(Yang <i>et al.</i> , 2019)
<i>Comamonas</i> sp. pw-6	150	24 h, 25 °C, 160 rpm	89.84%	(Chen <i>et al.</i> , 2024)
<i>Fictibacillus phosphorivorans</i> MJ9	52.22 ± 1.1	72 h, 35 °C	80.4 ± 1.1%	This study



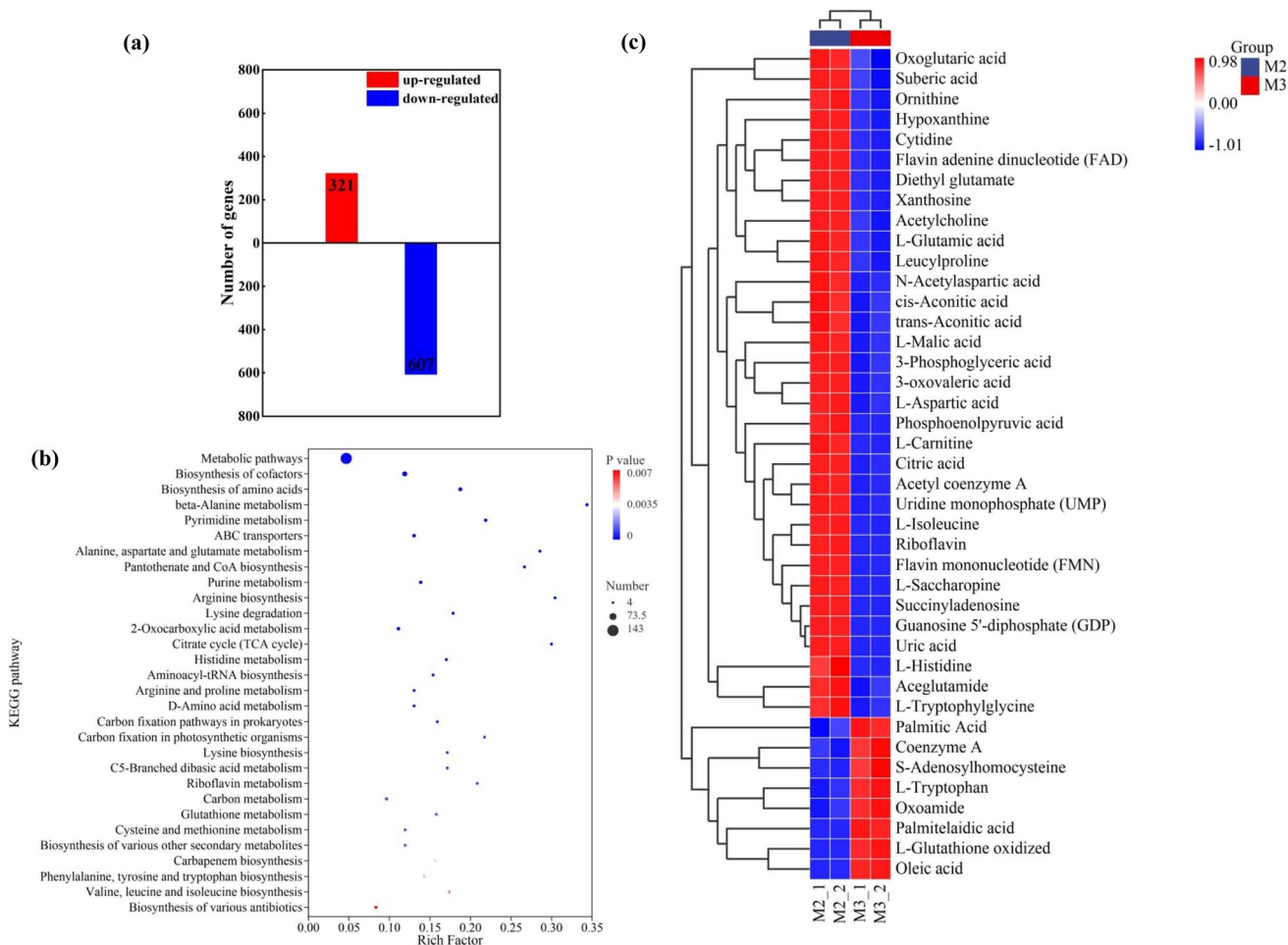


Fig. 3 (a) Number of differential metabolites before and after reaction, (b) KEGG enrichment analysis factor map, (c) differential metabolite heatmap.

degradable carbon source, rapidly produces pyruvate and Nicotinamide adenine dinucleotide (NADH), significantly increasing intracellular reducing power.<sup>35</sup> Down-regulation of phosphoenolpyruvate and 3-phosphoglyceric acid among the differential metabolites was observed, possibly due to the rapid depletion of glucose, resulting in a decrease in glycolytic intermediates. Malic acid (L-malic acid) and citric acid, both intermediates of the tricarboxylic acid cycle, were down-regulated, suggesting that carbon sources are preferentially used to provide reducing power (e.g., NADH) to drive nitrate reduction. This is because the cell meets its energy demands during DNRA primarily through reduction reactions, which require a large number of electrons for nitrate reduction. As a result, the cell may regulate its metabolic flow to meet this demand.<sup>36</sup> Coenzyme A (CoA) plays a key role in fatty acid  $\beta$ -oxidation, which was up-regulated, possibly indicating enhanced fatty acid  $\beta$ -oxidation to provide ATP for DNRA.<sup>37</sup> During DNRA, the electron transport chain may lead to the accumulation of reactive oxygen species (ROS), which can be toxic to the cell. In response, the cell may activate antioxidant mechanisms, as indicated by the up-regulation of oxidized glutathione. This suggests that the cell is undergoing an oxidative stress response to scavenge

excess ROS.<sup>38</sup> Additionally, tryptophan was up-regulated, which may enhance the cell's antioxidant capacity. Tryptophan acts as an antioxidant to alleviate ROS stress and also participates in the synthesis of stress proteins to help the cell cope with oxidative stress.<sup>39</sup> S-Adenosylhomocysteine (SAH) was also up-regulated, possibly reflecting methylation stress due to ROS accumulation from enhanced DNRA activity.<sup>40</sup> During the experiments, nitrite nitrogen accumulation was detected in the treated wastewater, which may be due to insufficient denitrifying enzyme activity or competition between DNRA and electron donors for denitrification. Denitrifying enzymes (e.g., Nir, Nos) depend on flavin coenzymes, such as flavin adenine dinucleotide (FAD) and flavin mononucleotide (FMN), to facilitate the reduction process. Down-regulation of both FAD and FMN was observed. This could limit the efficiency of electron chain transfer, reducing denitrifying enzyme activity and resulting in incomplete denitrification.<sup>41</sup> Additionally, the assimilation pathway that reduces nitrate to ammonium and integrates it into glutamate or glutamine was down-regulated for glutamate, which may indicate abnormal nitrogen assimilation. Therefore, nitrate reduction in this case may occur *via* the heterotrophic pathway, accompanied by incomplete denitrification.



### 3.3. Proteomics analysis

The differential proteins after 72 hours of anaerobic treatment of pickling wastewater by strain MJ9 are shown in Fig. 4a. A total of 275 differential proteins were identified, with 162 up-regulated and 113 down-regulated after the metabolism of strain MJ9 ( $p < 0.05$ ). Among these 275 significant metabolic proteins, 40 proteins related to  $\text{NO}_3^-$  reduction were selected for heatmap plotting, as shown in Fig. 4b.

A substantial amount of ATP is required to drive nitrate reduction to ammonium *via* the DNRA pathway. Post-reaction analysis revealed the upregulation of several proteins involved in nucleotide biosynthesis (as shown in Fig. 4c), including phosphoribosylformylglycinamide synthase (PurL), phosphoribosylformylglycinamide cyclo-ligase (PurM), phosphoribosylaminoimidazolesuccinocarboxamide synthase (PurC), and phosphoribosylglycinamide formyltransferase

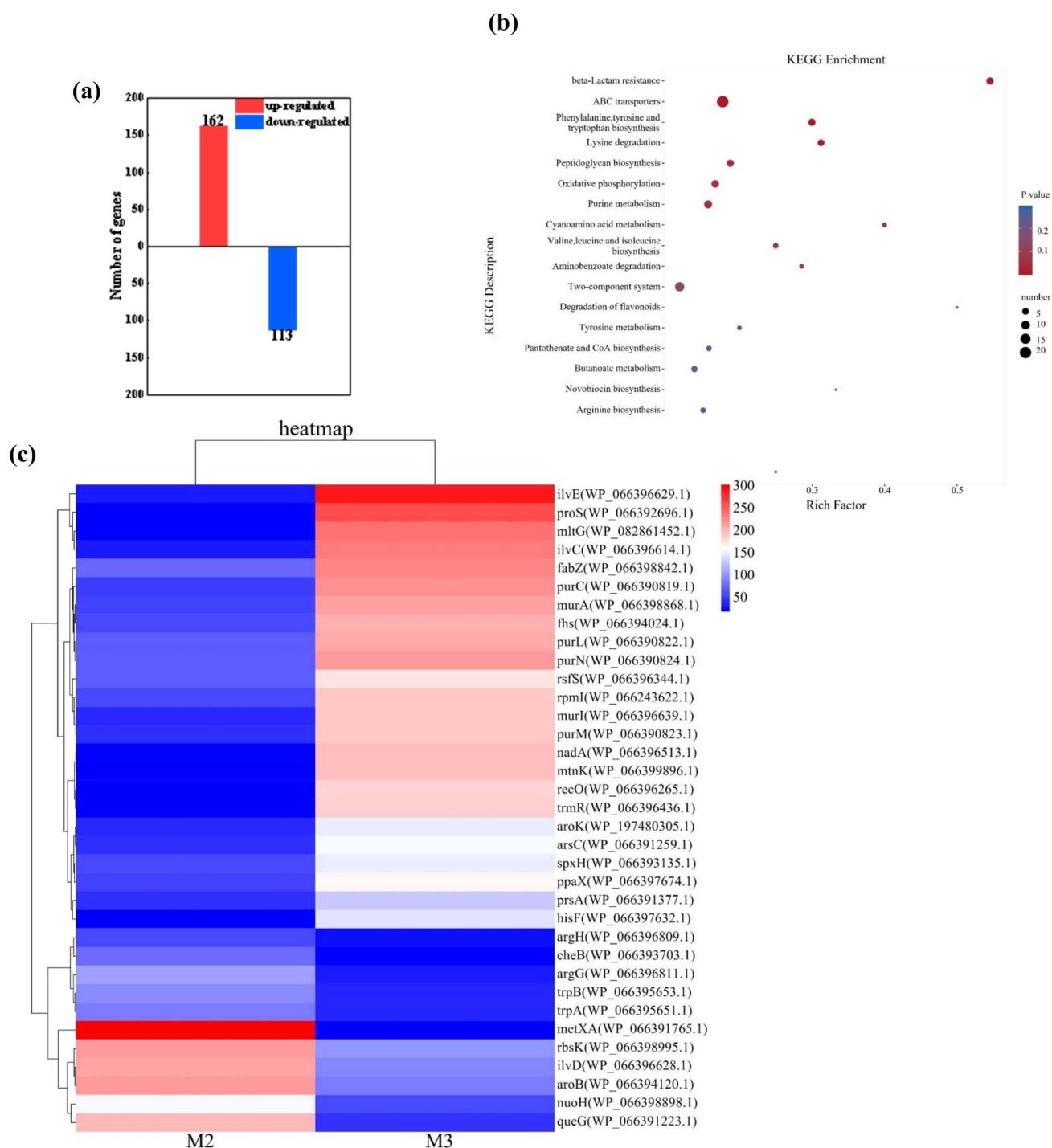
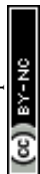


Fig. 4 (a) Number of up- and down-regulated proteins of biological process (BP). (b) DEPs within the BP in the groups classified using the gene ontology (GO) database. (c) Pathway classification based on KEGG enrichment analysis of DEPs in the group.



(PurN). In the purine metabolic pathway, the upregulation of these enzymes may enhance nucleotide production, thereby supporting increased ATP synthesis necessary for DNRA.<sup>42</sup> Moreover, downregulation of NADH-quinone oxidoreductase subunit H (NuoH) may reduce electron transport chain activity, resulting in the accumulation of NADH. This is beneficial, as NADH serves as a critical electron donor in nitrate reduction reactions, providing the necessary reducing power for DNRA.<sup>43</sup> In terms of fatty acid metabolism, upregulation of 3-hydroxyacyl-[acyl-carrier-protein] dehydratase (FabZ) was observed, which may promote the synthesis of fatty acids such as palmitic acid. This is supported by the metabolomic detection of elevated levels of palmitic acid and coenzyme A, indicating increased fatty acid biosynthetic activity.<sup>44</sup> Nicotinamide adenine dinucleotide (NAD), another key molecule in energy and redox metabolism, is synthesized more actively as evidenced by the upregulation of quinolinate synthase (NadA), suggesting enhanced NAD production to support more efficient nitrate reduction reactions.<sup>45</sup> Additionally, SpxH—a key regulator of the oxidative stress response—was found to be upregulated, potentially indicating that cells are mitigating reactive oxygen species (ROS) damage through enhanced antioxidant defenses.<sup>46</sup> However, critical denitrification enzymes such as nitrite reductase (NirS) and nitrous oxide reductase (NosZ) were not detected, suggesting that denitrification was not the dominant nitrate reduction pathway in this system. Furthermore, proteins associated with arginine biosynthesis, such as argininosuccinate lyase (ArgH) and argininosuccinate synthase (ArgG), were downregulated. This may reflect suppressed urea

cycle activity and reduced ammonium assimilation, further supporting the notion that assimilation pathways played a minimal role under the studied conditions.<sup>47</sup> Proteins associated with cell wall synthesis were also found to be upregulated, including UDP-*N*-acetylglucosamine 1-carboxyvinyltransferase (MurA) and glutamate racemase (MurI). This upregulation may be linked to the elevated metabolic demands required for nitrate reduction, where cell wall remodeling could facilitate enhanced material transport and energy metabolism. Additionally, in a neutral pH environment, such remodeling may play a role in regulating osmotic pressure, thereby contributing to the maintenance of cellular stability and metabolic homeostasis.<sup>48</sup> Furthermore, the upregulation of formate tetrahydrofolate ligase (Fhs) suggests a potential role in C1 metabolism, contributing to NADH regeneration or facilitating formate utilization. This may indirectly support the electron supply necessary for DNRA processes, further enhancing microbial nitrate reduction efficiency.<sup>49</sup>

The metabolic differentials and differentially expressed proteins were integrated into the KEGG database to construct a metabolic–protein interaction network, as illustrated in Fig. 5. Under anaerobic conditions, strain MJ9 appears to primarily reduce nitrate *via* dissimilatory nitrate reduction to ammonium (DNRA) and partial denitrification. This dual-pathway activity results in the accumulation of ammonium and nitrite nitrogen in the early stages. As the reaction progresses, strain MJ9 may utilize endogenous reserves or intracellular metabolites to further reduce nitrite to nitrogen gas (N<sub>2</sub>), while simultaneously assimilating a limited portion of ammonium nitrogen. This

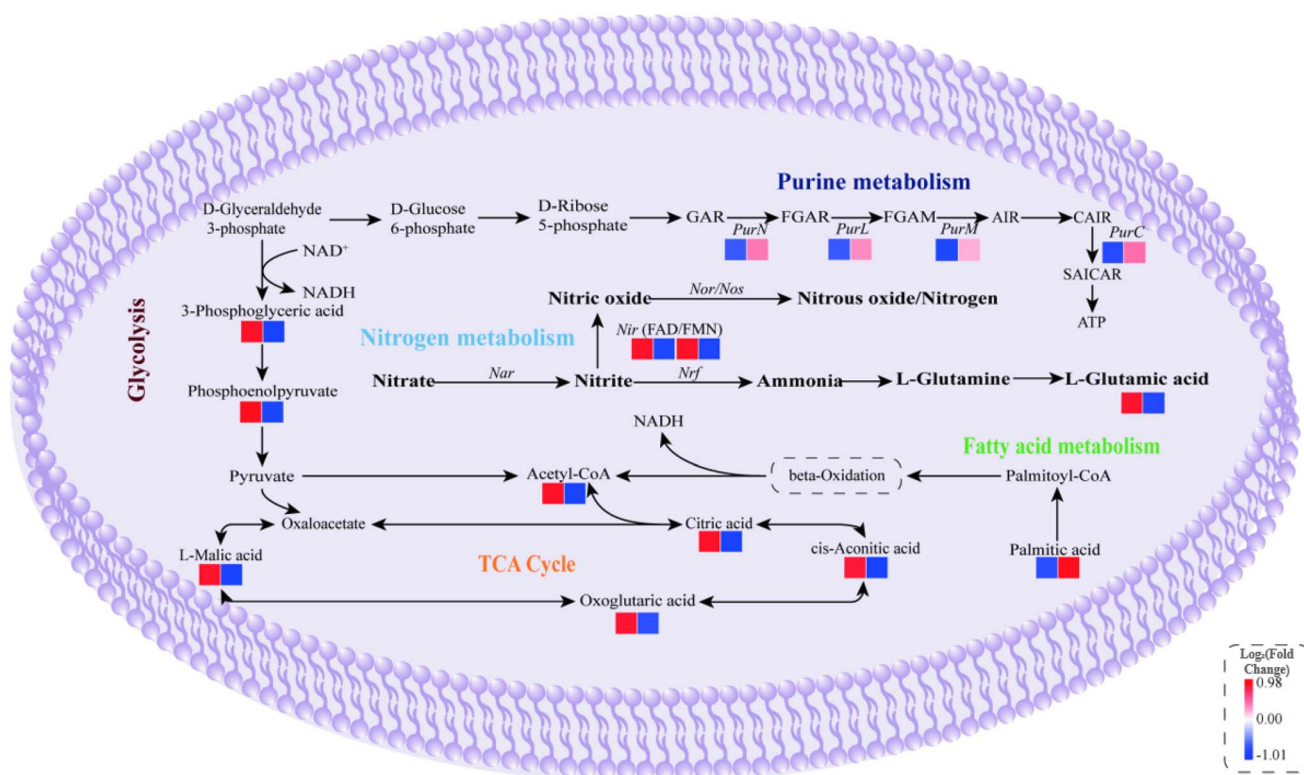


Fig. 5 Nitrogen metabolism pathway and acid tolerance mechanism of strain MJ9.



suggests a dynamic shift in metabolic strategy that balances energy generation, redox requirements, and nitrogen transformation under anaerobic stress. To investigate the metabolic mechanisms of wastewater treatment by strain MJ9, metabolic profiles before and after the reaction were compared. In glycolysis, phosphoenolpyruvic acid and 3-phosphoglyceric acid were downregulated, likely due to rapid glucose depletion reducing glycolytic intermediates. Intermediates of the tricarboxylic acid (TCA) cycle, malic acid (*l*-malic acid) and citric acid, were also downregulated, suggesting carbon sources were preferentially diverted to generate reducing power (*e.g.*, NADH) necessary for nitrate reduction. This reflects the cell's energy demands during dissimilatory nitrate reduction to ammonium (DNRA), which requires substantial electron supply, prompting metabolic regulation to meet these needs.<sup>50</sup> In fatty acid metabolism, palmitic acid was upregulated, possibly to promote fatty acid synthesis. These fatty acids undergo  $\beta$ -oxidation to produce acetyl-CoA, which feeds into the TCA cycle to generate ATP and NADH.<sup>51</sup> Additionally, the assimilation pathway—where nitrate is reduced to ammonium and incorporated into glutamate or glutamine—was indicated to be downregulated *via* decreased glutamate levels. This observation suggests a suppression of nitrogen assimilation processes under the tested conditions. Collectively, these results imply that nitrate reduction predominantly proceeds through DNRA, and accompanied by incomplete denitrification.

### 3.4. Integrated multi-omics analysis

To obtain a cohesive understanding of the metabolic state of strain MJ9, we integrated the metabolomic (Fig. 3) and proteomic (Fig. 4) datasets. This joint analysis revealed a consistent picture of cellular adaptation (Fig. 5). The upregulation of proteins involved in purine metabolism (PurL, PurM) and fatty acid synthesis (FabZ) correlated with the accumulation of key metabolites like palmitic acid and CoA (Fig. 3c; Fig. 4c), underscoring an enhanced demand for ATP and membrane lipid synthesis. This increased energy and membrane regeneration capacity is likely essential to maintain the activity of membrane-bound nitrate reductases and proton gradients under acidic stress. Concurrently, the downregulation of TCA cycle intermediates (malic acid, citric acid) at the metabolite level (Fig. 3c), coupled with the proteomic evidence of redirected electron flow (NuoH downregulation) (Fig. 4b), strongly supports a metabolic model where carbon flux is shunted to generate reducing equivalents (NADH) to fuel the energetically demanding DNRA pathway (Fig. 5), rather than for complete oxidative phosphorylation. This redirection ensures a sustained supply of NADH for nitrate/nitrite reduction, enabling strain MJ9 to use nitrate as an electron acceptor even under carbon-limited or acidic conditions, which would otherwise inhibit complete denitrification.

However, the upregulation of fatty acid synthesis and cell wall biosynthesis is a common bacterial stress response; whether strain MJ9 possesses unique acid-tolerance adaptations remains to be determined. It should also be noted that direct evidence for DNRA (*e.g.*, NrfA detection, <sup>15</sup>N tracing) is

lacking; therefore, we conclude that DNRA and partial denitrification likely coexist.

### 3.5. Limitations of the current study

While this study provides a system-level view of strain MJ9's adaptive strategies under extreme acidity (pH 3.1), we acknowledge several limitations that should be addressed in future work.

First, several control experiments essential for rigorous causal inference—including heat-inactivated cell controls, pH gradient controls, and aerobic controls—were not performed. Second, the inoculum dosage was quantified by centrifugation volume rather than cell density, and initial OD<sub>600</sub> values were not recorded. Third, the inference of DNRA as a major pathway is based on ammonium accumulation and absence of denitrification enzymes, rather than direct evidence such as NrfA detection, <sup>15</sup>N tracing, or gas product quantification. Additionally, key enzyme activities (*e.g.*, nitrate reductase Nar, nitrite reductase Nir, NADH oxidase) were not directly assayed or validated by western blot. Fourth, advanced multi-omics integration (*e.g.*, protein-metabolite correlation networks, metabolic flux analysis) was not conducted in this study; further investigations incorporating these approaches are needed to validate the proposed metabolic model. These limitations do not invalidate our main conclusions but highlight important directions for future mechanistic studies.

## 4 Conclusion

The acid-tolerant *Fictibacillus phosphorivorans* strain MJ9, newly isolated from sludge, exhibited excellent NO<sub>3</sub><sup>-</sup>-N removal specifically in highly acidic wastewater (pH 3.1). Metabolomic and proteomic analyses revealed that MJ9 resists this extreme acidity by upregulating energy and membrane synthesis while redirecting carbon flux to generate NADH for nitrate reduction *via* DNRA. This incomplete reduction, however, results in nitrite and ammonium accumulation, which in practice may require a post-treatment step to meet total nitrogen discharge limits. These findings highlight MJ9's potential for acidic wastewater treatment while identifying the need to manage its byproducts.

## Ethics approval

No ethical approval was required as it did not involve the collection or analysis of data involving human or animal subjects.

## Consent for publication

All authors read and approved the final manuscript.

## Funding

This work was supported by a grant from Changzhou Longcheng Talent Program (CQ20210092), Changzhou Sci&Tech Program (CJ20241080), National Natural Science Foundation of



China (no. 52400082), The Scientific Research Foundation of Jiangsu University of Technology, China (KYY20011).

## Author contributions

All authors contributed to the study conception and design. Jing Zhang contributed to visualization, investigation, software, project administration, writing – review & editing. Feifei Wang contributed to software, methodology, writing – original draft, writing – review & editing. Min Ai contributed to visualization, investigation, software, project administration, writing – review & editing. Xiafei Yin contributed to visualization, investigation, software, project administration, writing – review & editing. Lixue Liu contributed to data curation, investigation, writing – review & editing. Hefei Shi contributed to resources, supervision, validation. Guobin Liang contributed to supervision, validation. All authors read and approved the final manuscript.

## Conflicts of interest

The authors declare that they have no known competing financial interests or personal relationships that could have appeared to influence the work reported in this paper.

## Data availability

All data generated or analysed during this study are included in this published article and its supplementary information files. The data are available from the corresponding author upon reasonable request. Supplementary information (SI) is available. See DOI: <https://doi.org/10.1039/d6ra01143h>.

## References

- 1 R. Picetti, M. Deeney, S. Pastorino, *et al.*, Nitrate and nitrite contamination in drinking water and cancer risk: A systematic review with meta-analysis, *Environ. Res.*, 2022, **210**, 112988.
- 2 L. Yan, C. Wang, J. Jiang, *et al.*, Nitrate removal by alkali-resistant *Pseudomonas* sp. XS-18 under aerobic conditions: Performance and mechanism, *Bioresour. Technol.*, 2022, **344**, 126175.
- 3 B. Singh and C. Eric, Fertilizers and nitrate pollution of surface and ground water: an increasingly pervasive global problem, *SN Appl. Sci.*, 2021, **3**, 4.
- 4 Z. Lisheng, F. Menghan, Z. Di, *et al.*, La-Ca-quaternary amine-modified straw adsorbent for simultaneous removal of nitrate and phosphate from nutrient-polluted water, *Sep. Purif. Technol.*, 2023, **304**, 122248.
- 5 L. Jian, S. Junfeng, A. Amjad, *et al.*, Role of porous polymer carriers and iron-carbon bioreactor combined micro-electrolysis and biological denitrification in efficient removal of nitrate from wastewater under low carbon to nitrogen ratio, *Bioresour. Technol.*, 2021, **321**, 124447.
- 6 X. Liu, M. Huang, S. Bao, *et al.*, Nitrate removal from low carbon-to-nitrogen ratio wastewater by combining iron-based chemical reduction and autotrophic denitrification, *Bioresour. Technol.*, 2020, **301**, 122731.
- 7 V. Faust, T. A. Van Alen, H. J. M. Op Den Camp, *et al.*, Ammonia oxidation by novel "Candidatus Nitrosacidococcus urinae" is sensitive to process disturbances at low pH and to iron limitation at neutral pH, *Water Res.: X*, 2022, **17**, 100157.
- 8 H. Xi, X. Zhou, M. Arslan, *et al.*, Heterotrophic nitrification and aerobic denitrification process: Promising but a long way to go in the wastewater treatment, *Sci. Total Environ.*, 2022, **805**, 150212.
- 9 D. Li, F. X. Zeng, S. W. Yang, *et al.*, Simultaneous endogenous partial denitrification/anammox process for low-strength wastewater treatment: Process optimization, nitrogen removal and microbial dynamics, *Biochem. Eng. J.*, 2025, **213**, 11.
- 10 C. Y. Wang, F. Gao, S. Gao, *et al.*, Upflow blanket filter anammox (UBFA) system treating low-nitrogen wastewater: high-efficient nitrogen removal, granules formation, N<sub>2</sub>O emission, and microbial succession, *Bioprocess Biosyst. Eng.*, 2025, **48**, 395–412.
- 11 Q. Wu, T. He, X. Xu, *et al.*, Efficient removal of nitrate and ammonium by strain *Pseudomonas poae* EH-E3 under acidic pH and low-temperature conditions, *Environ. Technol. Innovat.*, 2024, **36**, 103858.
- 12 Q. Wu, T. He, M. Chen, *et al.*, Nitrogen removal characterization and functional enzymes identification of a hypothermia bacterium *Pseudomonas fragi* EH-H1, *Bioresour. Technol.*, 2022, **365**, 128156.
- 13 Y. M. Xie, X. L. Tian, Y. He, *et al.*, Nitrogen removal capability and mechanism of a novel heterotrophic nitrification-aerobic denitrification bacterium *Halomonas* sp. DN3, *Bioresour. Technol.*, 2023, **387**, 10.
- 14 X. Kang, X. X. Zhao, X. S. Song, *et al.*, Nitrogen removal by a novel strain *Priestia aryabhatai* KX-3 from East Antarctica under alkaline pH and low-temperature conditions, *Process Biochem.*, 2023, **130**, 674–684.
- 15 H. Chen, W. Zhou, S. Zhu, *et al.*, Biological nitrogen and phosphorus removal by a phosphorus-accumulating bacteria *Acinetobacter* sp. strain C-13 with the ability of heterotrophic nitrification-aerobic denitrification, *Bioresour. Technol.*, 2021, **322**, 124507.
- 16 X. Ke, C. Liu, S.-Q. Tang, *et al.*, Characterization of *Acinetobacter indicus* ZJB20129 for heterotrophic nitrification and aerobic denitrification isolated from an urban sewage treatment plant, *Bioresour. Technol.*, 2022, **347**, 126423.
- 17 L. Zeng, Z. Si, X. Zhao, *et al.*, Metabolome analysis of the response and tolerance mechanisms of *Saccharomyces cerevisiae* to formic acid stress, *Int. J. Biochem. Cell Biol.*, 2022, **148**, 106236.
- 18 A. Khalili, A. Ramesh, M. P. Sharma and P. H. Soil Rhizosphere, Enzymatic and Microbial Activities Under Different Nitrogen and Sulfur Fertilization of Soybean (*Glycine max* L.), *J. Soil Sci. Plant Nutr.*, 2024, **24**, 3986–3999.
- 19 X. Wang, Q. Li, Y. Zhang, *et al.*, Acid-tolerant denitrifying bacteria in low pH soils: diversity, activity and functional genes, *Appl. Environ. Microbiol.*, 2021, **87**, e02911.



- 20 H. Zhao, M. Liu, J. Chen, *et al.*, Molecular mechanisms of acid tolerance in anaerobic bacteria revealed by transcriptomics and metabolomics, *Microb. Cell*, 2022, **9**, 100–115.
- 21 P. Jiang, L. Sun, T. Yang, *et al.*, Integrated proteomic and metabolomic analysis of microbial stress adaptation under acidic anaerobic conditions, *Metabolites*, 2020, **10**, 506.
- 22 J. Zhen, H. Ma, Y. Wu, *et al.*, Nitrogen elimination by a novel salt-tolerant bacterium *Alcaligenes aquatilis* DN-1: Characteristics and resistance mechanism of the strain, *J. Water Proc. Eng.*, 2025, **73**, 107412.
- 23 C. R. Liu, C. Y. Zhao, L. J. Wang, *et al.*, Biodegradation mechanism of chlorpyrifos by *Bacillus* sp. H27: Degradation enzymes, products, pathways and whole genome sequencing analysis, *Environ. Res.*, 2023, **239**, 12.
- 24 SEPA, *Water and Wastewater Monitoring Analysis Method*, 4th edn, China Environmental Science Press, Beijing, 2002.
- 25 M. Kanehisa, M. Furumichi, Y. Sato, *et al.*, KEGG for taxonomy-based analysis of pathways and genomes, *Nucleic Acids Res.*, 2023, **51**, D587–D592.
- 26 X. Zeng, Q. Pan, Y. Guo, *et al.*, Potential mechanism of nitrite degradation by *Lactobacillus fermentum* RC4 based on proteomic analysis, *J. Proteomics*, 2019, **194**, 70–78.
- 27 V. Jha, N. A. Dafale, Z. Hathi, *et al.*, Genomic and functional potential of the immobilized microbial consortium MCST-1 for wastewater treatment, *Sci. Total Environ.*, 2021, **777**, 146110.
- 28 J. Wang, D. Zhu, S. Zhao, *et al.*, Effect of liquid volume and microflora source on degradation rate and microbial community in corn stover degradation, *AMB Express*, 2021, **11**, 80.
- 29 J. Xu, X. Liu, J. Huang, *et al.*, The contributions and mechanisms of iron-microbes-biochar in constructed wetlands for nitrate removal from low carbon/nitrogen ratio wastewater, *RSC Adv.*, 2020, **10**, 23212–23220.
- 30 F. Huang, R. R. R. Sardari, A. Jasilionis, *et al.*, Cultivation of the gut bacterium *Prevotella copri* DSM 18205T using glucose and xylose as carbon sources, *MicrobiologyOpen*, 2021, **10**, e1213.
- 31 Q. Yang, T. Yang, Y. Shi, *et al.*, The nitrogen removal characterization of a cold-adapted bacterium: *Bacillus simplex* Hb, *Bioresour. Technol.*, 2021, **323**, 124554.
- 32 C. Li, J. Yang, X. Wang, *et al.*, Removal of nitrogen by heterotrophic nitrification-aerobic denitrification of a phosphate accumulating bacterium *Pseudomonas stutzeri* YG-24, *Bioresour. Technol.*, 2015, **182**, 18–25.
- 33 J.-R. Yang, Y. Wang, H. Chen, *et al.*, Ammonium removal characteristics of an acid-resistant bacterium *Acinetobacter* sp. JR1 from pharmaceutical wastewater capable of heterotrophic nitrification-aerobic denitrification, *Bioresour. Technol.*, 2019, **274**, 56–64.
- 34 M. X. Chen, Y. J. Li, L. Wu, *et al.*, Optimal conditions and nitrogen removal performance of aerobic denitrifier *Comamonas* sp. pw-6 and its bioaugmented application in synthetic domestic wastewater treatment, *Water Sci. Technol.*, 2024, **89**, 3007–3020.
- 35 J. Liu, J. Li, H.-D. Shin, *et al.*, Protein and metabolic engineering for the production of organic acids, *Bioresour. Technol.*, 2017, **239**, 412–421.
- 36 A. U. Igamberdiev and A. T. Eprintsev, Organic Acids: The Pools of Fixed Carbon Involved in Redox Regulation and Energy Balance in Higher Plants, *Front. Plant Sci.*, 2016, **7**, 1042.
- 37 M. J. Torres, J. Simon, G. Rowley, *et al.*, Nitrous Oxide Metabolism in Nitrate-Reducing Bacteria: Physiology and Regulatory Mechanisms, *Adv. Microb. Physiol.*, 2016, **68**, 353–432.
- 38 R. Mcminimy, A. G. Manford, C. L. Gee, *et al.*, Reactive oxygen species control protein degradation at the mitochondrial import gate, *Mol. Cell*, 2024, **84**, 31.
- 39 O. S. Adeyemi, J. I. Obeme-Imom, B. O. Akpor, *et al.*, Altered redox status, DNA damage and modulation of L-tryptophan metabolism contribute to antimicrobial action of curcumin, *Heliyon*, 2020, **6**, e03495.
- 40 T. Y. Gao, C. Y. Lai and H. P. Zhao, Riboflavin-mediated interspecies electron transfer in a H<sub>2</sub>-based denitrifying biofilm, *J. Water Proc. Eng.*, 2024, **66**, 10.
- 41 K. Soda, Overview of Polyamines as Nutrients for Human Healthy Long Life and Effect of Increased Polyamine Intake on DNA Methylation, *Cells*, 2022, **11**, 1.
- 42 J. H. Peng, S. C. Lo, Y. N. Yu, *et al.*, Carbon fluxes rewiring in engineered *E. coli* via reverse tricarboxylic acid cycle pathway under chemolithotrophic condition, *J. Biol. Eng.*, 2025, **19**, 17.
- 43 C. Wang and S. Qiao, Electron transfer mechanism of intracellular carbon-dependent DNRA inside anammox bacteria, *Water Res.*, 2023, **244**, 9.
- 44 A. Ganesh Kumar, N. C. Mathew, K. Sujitha, *et al.*, Publisher Correction: Genome analysis of deep sea piezotolerant *Nesiotobacter exalbescens* COD22 and toluene degradation studies under high pressure condition, *Sci. Rep.*, 2020, **10**, 18815.
- 45 Z. Y. Guo, L. Wang and C. Y. Yu, Over-expressing *NadA* quinolinate synthase in *Escherichia coli* enhances the bioelectrochemistry in microbial fuel cells, *Biol. Open*, 2023, **12**, 5.
- 46 H. Schafer, A. Heinz, P. Sudzinova, *et al.*, *Spx*, the central regulator of the heat and oxidative stress response in *B. subtilis*, can repress transcription of translation-related genes, *Mol. Microbiol.*, 2019, **111**, 514–533.
- 47 Z. M. Xie, C. M. Chen, Y. Tian, *et al.*, Transcriptional profiling reveals the effect of arginine on *Actinobacillus succinogenes* growth and fermentation, *World J. Microbiol. Biotechnol.*, 2025, **41**, 12.
- 48 S. Garde, P. K. Chodisetti and M. Reddy, Peptidoglycan: Structure, Synthesis, and Regulation, *EcoSal Plus*, 2021, **9**, 2.
- 49 X. Wang, Q. Li, Y. Zhang, *et al.*, Acid-tolerant denitrifying bacteria in low pH soils: diversity, activity and functional genes, *Appl. Environ. Microbiol.*, 2021, **87**, e02911.
- 50 C. Wang and S. Qiao, Electron transfer mechanism of intracellular carbon-dependent DNRA inside anammox bacteria, *Water Res.*, 2023, **244**, 120443.
- 51 V. Pavoncello, F. Barras and E. Bouveret, Degradation of exogenous fatty acids in *Escherichia coli*, *Biomolecules*, 2022, **12**, 1019.

